

ORIGINAL ARTICLE

Human Umbilical Cord-Derived Mesenchymal Stem Cells Repair SU5416-Injured Emphysema by Inhibiting Apoptosis via Rescuing VEGF-VEGFR2-AKT Pathway in Rats

Qin Chen¹, Lu Lv², Chujie Zheng³, Huiwen Pan², Jili Xu³, Jiang Lin¹, Zhaoqun Deng¹, Wei Qian³

¹Laboratory Center, Affiliated People's Hospital of Jiangsu University, Zhenjiang, China

²Department of Cardiothoracic Surgery, Affiliated People's Hospital of Jiangsu University, Zhenjiang, China

³Department of Otolaryngology-Head and Neck Surgery, Affiliated People's Hospital of Jiangsu University, Zhenjiang, China

Background and Objectives: Chronic obstructive pulmonary disease (COPD) is a common, frequently-occurring disease and poses a major health concern. Unfortunately, there is current no effective treatment for COPD, particularly emphysema. Recently, experimental treatment of COPD using mesenchymal stem cells (MSCs) mainly focused on bone marrow-derived MSCs (BM-MSCs). Human umbilical cord-derived MSCs (hUC-MSCs) have more advantages compared to BM-MSCs. However, studies on the role of hUC-MSCs in management of COPD are limited. This study sought to explore the role of hUC-MSCs and its action mechanisms in a rat model of VEGF receptor blocker SU5416-injured emphysema.

Methods and Results: hUC-MSCs were characterized by immunophenotype and differentiation analysis. Rats were divided into four groups: Control, Control+MSC, SU5416 and SU5416+MSC. Rats in model group were administered with SU5416 for three weeks. At the end of the second week after SU5416 administration, model group were infused with 3×10^6 hUC-MSCs through tail vein. After 14 days from hUC-MSCs transplantation, rats were euthanized and data were analyzed. HE staining and mean linear intercepts showed that SU5416-treated rats exhibited typical emphysema while emphysematous changes in model rats after hUC-MSCs transplantation disappeared completely and were restored to normal phenotype. Furthermore, hUC-MSCs inhibited apoptosis as shown by TUNEL and Western blotting. ELISA and Western blotting showed hUC-MSCs rescued VEGF-VEGFR2-AKT pathway in emphysematous lungs.

Conclusions: The findings show that hUC-MSCs effectively repair the emphysema injury. This study provides the first evidence that hUC-MSCs inhibit apoptosis via rescuing VEGF- VEGFR2-AKT pathway in a rat model of emphysema.

Keywords: COPD, Emphysema, SU5416, hUC-MSCs, VEGF-VEGFR2-AKT pathway, Apoptosis

Received: September 2, 2021, Revised: January 19, 2022,
Accepted: January 24, 2022, Published online: February 28, 2022
Correspondence to **Wei Qian**

Department of Otolaryngology-Head and Neck Surgery, Affiliated
People's Hospital of Jiangsu University, Dianli RD. 8, Zhenjiang
212002, China

Tel: +86-511-88917833, Fax: +86-511-85234387

E-mail: dwqian@yahoo.com

© This is an open-access article distributed under the terms of the Creative Commons Attribution Non-Commercial License (<http://creativecommons.org/licenses/by-nc/4.0/>), which permits unrestricted non-commercial use, distribution, and reproduction in any medium, provided the original work is properly cited.

Copyright © 2022 by the Korean Society for Stem Cell Research

Introduction

Chronic obstructive pulmonary disease (COPD) is characterized by incompletely reversible airflow limitation. In addition, the characteristic pathological changes in COPD include small airway lesions and emphysema change. COPD is a common disease and is currently one of the leading causes of death globally (1). Patients with COPD usually suffer from complications such as muscle wasting, cardiovascular disease, depression, osteoporosis, and lung cancer (1). These complications result in high medical cost and social burden. Unfortunately, currently, there is

no effective therapeutic approach for preventing development or for treatment of COPD, particularly emphysema. Therefore, there is an urgent need to seek a new and effective treatment approach to decrease the heavy burden and high mortality of patients due to this disease.

Mesenchymal stem cells (MSCs) occur in various tissues including bone marrow, umbilical cord blood, umbilical cord tissue, placental tissue, and adipose tissue. Recent animal experiments and few clinical studies report that lung injury diseases including acute lung injury, bronchopulmonary dysplasia, pulmonary hypertension, asthma and COPD can effectively be treated by administration with MSCs (2-4). Currently, experimental treatment of MSCs for COPD and emphysema mainly focuses on bone marrow-derived MSCs (BM-MSCs). Although BM-MSCs are effective in emphysema models (5-7), the clinical application of BM-MSCs may be limited due to the high invasiveness and the fact that the function of MSCs declines with increase in the donors age (8). Therefore, it is important to explore activity of MSCs from other origins. Human umbilical cord-derived MSCs (hUC-MSCs) have more advantages in clinical application compared to BM-MSCs. For example, hUC-MSCs are easier to access without any invasiveness, can be efficiently expanded in labs, have lower immunogenicity, grow more rapidly, have faster doubling times and show a lower risk of infection (9-13), implying that hUC-MSCs are a better alternative for stem cell-based therapy. Several studies report that hUC-MSCs are effective in treatment of lung diseases such as radiation-induced lung injury, lung fibrosis, neonatal lung injury and severe COVID-19 (10-13). However, currently only a few papers report that hUC-MSCs are effective in treatment of COPD. A recent clinical study reported that UC-MSCs were safe and effective in improving the quality of life and clinical conditions of COPD patients (14). Findings from an animal experiment showed that hUC-MSCs had pulmonary regenerative effects in a COPD mouse model (15). Ridzuan et al. (16) reported that hUC-MSCs ameliorated airway inflammation in a COPD model of rats. Therefore, more studies should explore the effect and mechanisms of action of hUC-MSCs in treatment of this COPD to provide more experimental basis. The aim of this study was to explore the role of hUC-MSCs and its mechanisms of action in a rat model of SU5416-induced emphysema.

Materials and Methods

hUC-MSCs isolation and culture

The experimental protocol used in this study was ap-

proved by the Institutional Ethics Committee of the Affiliated People's Hospital of Jiangsu University (No. K-20210144-W). Fresh umbilical cords were obtained from healthy mothers attending the Affiliated People's Hospital of Jiangsu University. All the mothers that participated in this study signed written informed consent prior to the study. Umbilical cords were processed immediately after harvesting. Cords were washed twice with phosphate-buffered saline (PBS) in 1% penicillin and streptomycin and all blood vessels were removed before slicing them into 1-mm³ pieces. Small pieces of cords were placed on petri dishes and human umbilical cord mesenchymal stem cells complete medium (Cyagen, Guangzhou, China) was added to the samples. All tissues were maintained at 37°C with 5% CO₂ in a humidified incubator. The medium was replaced every 3 days and nonadherent cells were removed. When fibroblast-like cells reached about 80% confluence, they were detached from petri dishes using 0.25% trypsin (Gibco, USA) and passaged into new flasks for further expansion. Cells from the 3rd passage were used in subsequent experiments.

Characterization of hUC-MSCs

Immunophenotype and differentiation assay *in vitro* were carried out to characterize hUC-MSCs. Surface markers of hUC-MSCs were analyzed by flow cytometry (Aria II, Becton Dickson, USA). After the third passage, cells were treated with 0.25% trypsin and washed twice with PBS. Cells were then subjected to mouse anti-human monoclonal antibodies including three negative markers PE-CD11b, PE-CD19, PE-CD34 and three positive markers of PE-CD29, PE-CD73, PE-CD90 (BD, USA). Mouse PE-IgG was used as isotype control.

Osteogenic or adipogenic differentiation assay of hUC-MSCs was performed using the third passage cells. In brief, cells were cultured in a specific medium containing osteogenic (Cyagen) or adipogenic (STEMCELL, Canada) materials. The medium was changed every three days. After culturing for three to four weeks, osteogenic and adipogenic differentiation were determined by Alizarin Red staining and Oil Red O staining, respectively.

Animal studies

The experimental procedures were conducted under EC Directive 86/609/EEC for animal experiments and approved by the Institutional Animal Care and Use Committee of Jiangsu University (No. UJS-IACUC-2019040901). Our experiments conformed to the effective laws and ethical recommendations currently in China. Male Sprague-Dawley (SD) rats were purchased from Jiangsu University

and kept in the Laboratory Animal Research Center of Jiangsu University. Emphysema models were established using the VEGF receptor blocker, SU5416 as described previously (17). Rats were divided randomly into four groups: (A) Control group (CON, n=9), (B) Control+MSC group (CON+MSC, n=9), (C) SU5416 (SU, n=9) and (D) SU5416+MSC group (SU+MSC, n=9). Rats in group C and D were administered with SU5416 (Abcam, Cambridge, UK) subcutaneously at a dosage of 20 mg/kg body weight, three times a week for 3 weeks. SU5416 was dissolved in diluents containing 0.5% carboxymethyl-cellulose sodium, 0.9% sodium chloride, 0.4% polysorbate 80, and 0.9% benzyl alcohol in deionized water (17). Rats in group A and B only received the diluents administered subcutaneously. At the end of the second week after administration of SU5416 or diluents, 3×10^6 hUC-MSCs were administered into groups B and D, at the third passage resuspended in 0.3 ml PBS through the tail vein, whereas groups A and C received only 0.3 ml PBS.

Lung tissues and bronchoalveolar lavage fluid (BALF) processing

After 14 days from hUC-MSCs transplantation, rats were sacrificed. BALF and lung tissues were harvested. After cross-clamping the left lung, BALF was obtained by intratracheal insertion of a catheter and lavage with 1 ml of cold saline two times (final volume 2 ml) in the right lung. The left lungs were then harvested. The upper lobes of the left lungs were fixed in 4% paraformaldehyde for histological analysis and apoptosis assay, whereas the remaining left lungs were kept at -80°C for expression analysis. BALF was centrifuged at 2,000 rpm for 10 min and the supernatant was used for ELISA analysis.

Histological analysis of lung tissues

Paraformaldehyde-fixed lungs were paraffin-embedded, sectioned into 4 μm slices and stained with hematoxylin and eosin (HE) for histological analysis. Mean linear intercept (MLI) was calculated to determine the extent of emphysematous changes and the repair ability of hUC-MSCs in emphysema. Two random slices from each specimen were selected to determine the MLI. In brief, the slices were observed at original magnification of $\times 100$, and five fields of each slice avoiding large blood vessels and bronchial were used. A cross was drawn at the center of each field of vision, and the total number of alveolar septa (NS) encountered in all lines were counted. In addition, the total length of the crosshairs (L) was measured. MLI was calculated using the formula $\text{MLI} = \text{L}/\text{NS}$. The MLI value represented the average alveoli diameter.

TUNEL analysis

Apoptosis assay of lung tissues was performed using TUNEL method using paraffin sections. TUNEL assay was carried out with commercially available kit (Sigma-Aldrich, QIA33) following the manufacturer's instructions. Briefly, paraffin sections were deparaffinized and rehydrated. The slides were then digested with proteinase K (20 $\mu\text{g}/\text{ml}$) for 20 minutes and the digestion was stopped by addition of 3% H_2O_2 for 5 minutes. Sections were then covered with Equilibration Buffer for 30 minutes. Subsequently, sections were incubated with TdT Labeling Reaction Mixture in a humid atmosphere at 37°C for 90 minutes. Stop solution was added to the sections for 5 minutes to stop the reaction. Slides were then washed three times with TBS and incubated with conjugate for 30 minutes. After rinsing with TBS, sections were covered with DAB solution for 10 minutes. Slides were counterstained with hematoxylin. Apoptosis index was calculated by dividing the number of TUNEL-positive cells to the total cell number in randomly selected 10 fields at $\times 400$ magnification, and the result was multiplied by 100.

VEGF ELISA analysis

VEGF level in BALF was evaluated using the Rat VEGF Quantikine ELISA Kit (R&D, USA). 50 μl BALF was examined following the manufacturer's instructions. All standards and specimens were measured in duplicate. Analysed proteins included human and rat VEGF. The results were expressed as pg/ml .

Western blot analysis

Left lung tissues were lysed in RIPA lysis buffer (Beyotime, Shanghai, China). For detection of phosphorylated VEGF receptor 2 (p-VEGFR2) and phosphorylated AKT (p-AKT), phosphatase inhibitor (Biosharp) was also added in the lysis buffer to protect the phosphorylated groups. Protein concentration of each sample was determined using BCA protein assay kit (Beyotime, Shanghai, China). Total proteins were separated through a 12% sodium dodecyl sulfate polyacrylamide gel electrophoresis and transferred to polyvinylidene fluoride membranes. The membranes were then blocked in 5% bovine serum albumin for 2 h at room temperature and incubated with primary antibodies against caspase-3 (rabbit polyclonal IgG, 1 : 2,000) (Proteintech), PCNA (rabbit polyclonal IgG, 1 : 2,000) (Proteintech), VEGF (mouse monoclonal IgG2B, 1 : 1,000) (R&D), p-VEGFR2 (rabbit polyclonal IgG, 1 : 1,000) (Millipore), VEGFR2 (rabbit polyclonal IgG, 1 : 1,000) (Abcam), p-AKT (rabbit polyclonal IgG, 1 : 1,000) (Affinity), AKT (rabbit polyclonal IgG, 1 : 1,000) (Affinity)

and β -actin (rabbit polyclonal IgG, 1 : 1,000) (Abcam) overnight at 4°C. After washing three times with 0.1% PBST, the membranes were incubated with the appropriate horseradish peroxidase (HRP)-conjugated anti-mouse or anti-rabbit secondary antibody. Finally, the membranes were detected with enhanced chemiluminescence (Millipore, MA, USA). β -actin was used as the internal control for protein loading.

Measurement of pro-inflammatory cytokines by real-time PCR and ELISA

Real-time quantitative PCR (RQ-PCR) was performed on a 7500 Thermo cycler (Applied Biosystems, CA, USA). The primer sequences of expression were IL-1 β , 5'-GCTG TGCGAGCTACCTATGTCTTG-3' (forward), 5'-AGGTC GTCATCATCCCACGAG-3' (reverse); IL-6, 5'-CCACTTCAACAAGTCGAGGCTTA-3' (Forward), 5'-GTGCATCATCGCTGTTCATACAATC-3' (Reverse); TNF α , 5'-ATACA CTGGCCCGAGGCAAC-3' (Forward), 5'-CCACATCTCGGATCATGCTTTC-3' (Reverse) and β -ACTIN, 5'-AAGGCCAACCGTGAAAAGAT-3' (forward), 5'-GCTCGAAGCTAGGGCAACA-3' (reverse). The housekeeping gene β -ACTIN was used as reference sequence to calculate the abundance of target mRNA. Relative expression levels were determined by using the $2^{-\Delta\Delta Ct}$ method using β -ACTIN levels for normalization.

The rats IL-1 β , IL-6 and TNF α protein level in BALF was evaluated by the Quantikine ELISA Kit (R&D, USA) according to the manufacturer's manual.

Statistical analysis

GraphPad Prism 5.0 (GraphPad software, USA) was used for statistical analysis and for generation of figures. Data were presented as mean \pm SEM. Unpaired *t* test and one-way analysis of variance were performed to compare the difference among two or multiple groups, respectively. The level of statistical significance was set at $p < 0.05$ for all tests.

Results

Isolation and characterization of hUC-MSCs

After the first 3~5 days of initial culture, hUC-MSCs adhered to plastic surface, and presented a spindle fibroblast-like appearance. hUC-MSCs reached 80%~90% confluence approximately 15 days later. *In vitro* immunophenotype and differentiation assay of hUC-MSCs were carried out prior to experimental use. Flow cytometry analysis showed that hUC-MSCs were negative for CD11b, CD19, and CD34, but positive for CD29, CD73, and CD90 (Fig. 1A). Differentiation assays showed that hUC-MSCs retained the ability to differentiate into osteoblasts and adipocytes as shown by positive staining with Alizarin Red (Fig. 1Ba) and Oil Red O (Fig. 1Bb). Notably, the non-differentiated control did not show positive staining (Fig. 1Bc).

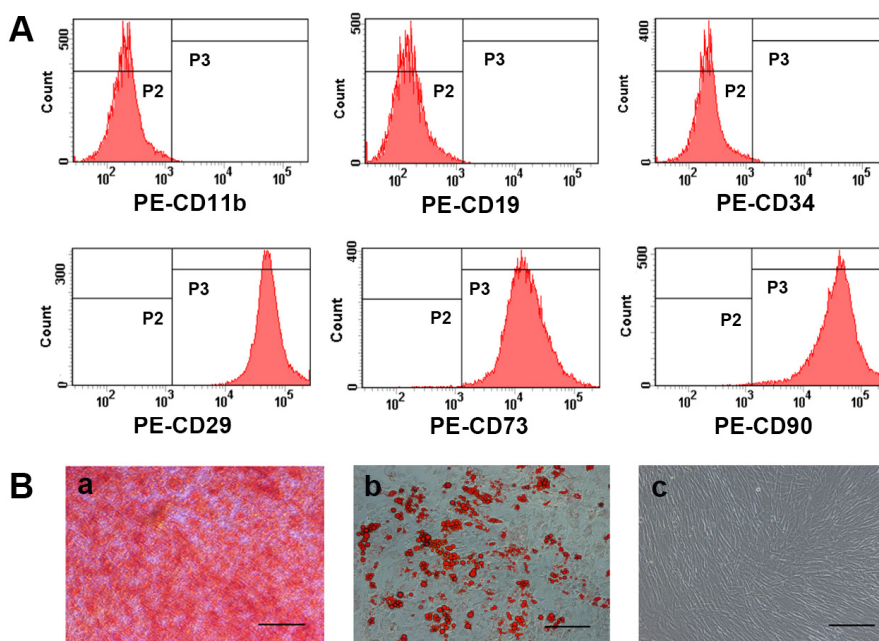


Fig. 1. Characterization of hUC-MSCs. (A) Flow cytometry analysis of surface antigens of hUC-MSCs. hUC-MSCs were negative for CD11b, CD19 and CD34, but positive for CD29, CD73 and CD90. (B) Differentiation potential of hUC-MSCs. (a) Osteogenic differentiation results using Alizarin Red staining, numerous cells became Alizarin Red positive. (b) Adipogenic differentiation results using Oil Red O staining, some of the cells contained numerous Oil Red O-positive lipid droplets. (c) Non-stimulated control cells grown in regular medium. (a~c) Magnification, $\times 100$; scale bar, 200 μ m.

hUC-MSCs repaired lung injury in SU5416-induced emphysema

Emphysema models were established by administration of SU5416 into SD rats three times per week for 3 weeks. After 14 days from the first administration with SU5416 or diluents, each rat in group B and D were administered with 3×10^6 hUC-MSCs through the tail vein. On day 28, rats were euthanized and tissues were harvested for further analysis. HE staining results indicated that rats in the SU5416 group had severe alveolar destruction and enlargement of the alveolar spaces compared with the control. This finding implies that the lungs had become emphysematous. However, emphysematous changes disappeared completely and were restored to the normal phenotype in SU5416-treated rats that received hUC-MSCs infusion. Notably, no difference in morphology was observed between samples from the rats in the Control+MSC group and those in the Control group (Fig. 2A). MLI was determined to quantify enlargement of the alveolar spaces. MLI was significantly higher in the SU5416 group ($94.46 \pm 6.60 \mu\text{m}$) compared with that in the Control group ($73.99 \pm 2.03 \mu\text{m}$, $p < 0.05$). However, MLI was restored to the normal level in the SU5416+MSC group ($74.65 \pm 3.69 \mu\text{m}$). This finding shows that hUC-MSCs transplantation can repair SU5416-induced emphysema completely. The Control group and the Control group with hUC-MSCs treatment showed no significant differences in MLI values, their MLI were $73.99 \pm 2.03 \mu\text{m}$ and $72.75 \pm 3.06 \mu\text{m}$, respectively (Fig. 2B).

hUC-MSCs inhibited apoptosis in SU5416-induced emphysema

To analyze the apoptosis of lung tissues, TUNEL staining and western blot for active caspase-3 were performed. TUNEL results showed that the apoptosis index of SU5416 group ($35.65 \pm 1.48\%$) was significantly higher compared with that of the Control group ($0.74 \pm 0.24\%$, $p < 0.0001$). However, the apoptosis index in the SU5416+MSC group ($0.96 \pm 0.43\%$) was significantly lower compared with that of the SU5416 group ($35.65 \pm 1.48\%$) ($p < 0.0001$) and returned to the normal level after administration of hUC-MSCs (Fig. 3A and 3B). Western blotting analysis showed that active caspase-3 was significantly higher in the SU5416 group compared with the Control group and it was significantly decreased in the SU5416+MSC group. No significant difference in caspase-3 activity was observed between the Control+MSC group and the Control group. Proliferation was not significantly changed for PCNA levels were similar in four groups (Fig. 3C).

hUC-MSCs rescued VEGF expression in SU5416-induced emphysema

To elucidate the mechanisms of action of hUC-MSCs in repairing lung injury in SU5416-induced emphysema, expression of VEGF protein in BALF and lung tissues were determined by ELISA and western blotting, respectively. Analysis showed that expression of VEGF was significantly decreased in SU5416-treated lungs compared with that in the Control group. Notably, expression of VEGF was significantly increased and restored to the normal level in the SU5416+MSC group (Fig. 4A and 4B). There was no significant difference in VEGF expression between the Control+MSC group and the Control group.

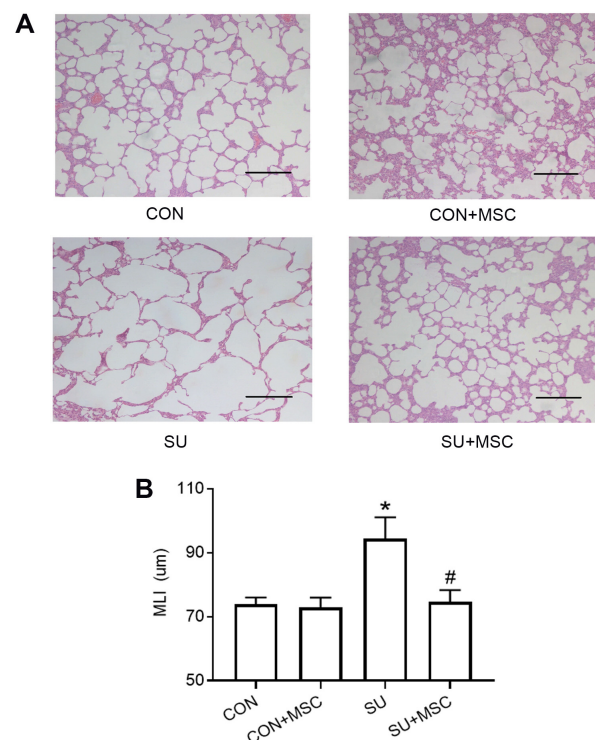


Fig. 2. hUC-MSCs repaired SU5416-induced emphysema. (A) Representative results of HE staining in lung sections chosen from each group. There was no significant difference between the Control group (CON) and the Control+MSC group (CON+MSC). Emphysematous changes were observed in the group treated with SU5416 (SU). hUC-MSCs transplantation repaired SU5416-induced emphysema (SU+MSC). Magnification, $\times 100$; scale bar, $200 \mu\text{m}$. (B) Morphometric analysis of the mean linear intercept (MLI). Values of MLI are presented as mean \pm SEM. * $p < 0.05$ compared with the Control group. # $p < 0.05$ compared with the SU5416 (SU) group. $n = 9$.

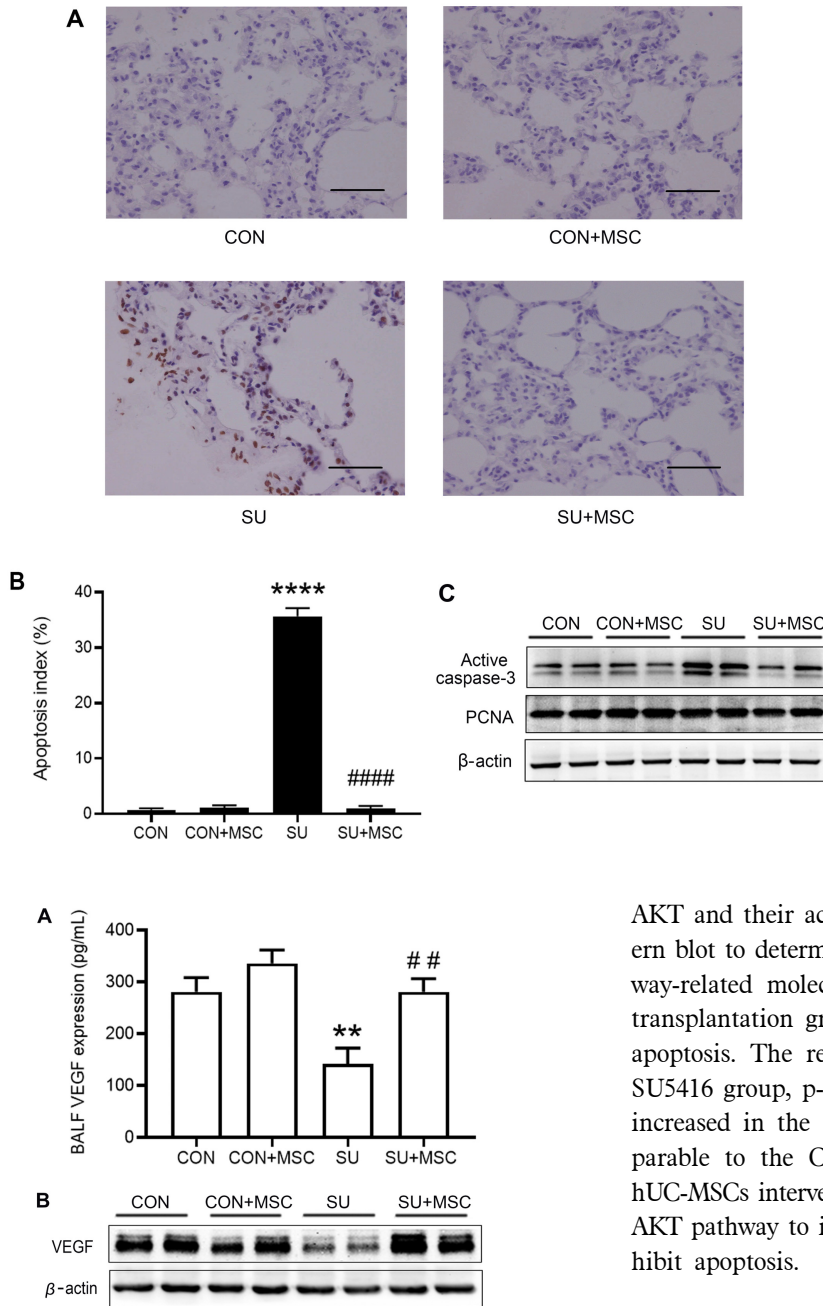


Fig. 4. hUC-MSCs rescued VEGF expression in SU5416-induced emphysema. (A) VEGF protein level in BALF was determined by ELISA. Data are presented as mean±SEM. **p<0.01 compared with the Control (CON) group, ##p<0.01 compared with the SU5416 (SU) group. n=9. (B) VEGF protein level in lungs as determined by western blotting.

hUC-MSCs activated VEGFR2 and AKT in SU5416-induced emphysema

The AKT survival signal mediated by VEGF and VEGF receptor 2 (VEGFR2) is essential for the survival of endothelial cells. We detected the expressions of VEGFR2,

Fig. 3. hUC-MSCs inhibited apoptosis of SU5416-treated lungs. (A) Representative results of TUNEL assay using lung sections chosen from each group. There was no significant difference between the Control (CON) group and the Control+MSC (CON+MSC) group. Increased TUNEL-positive cells were observed in the group treated with SU5416 (SU). hUC-MSCs reduced TUNEL-positive cells (SU+MSC). Magnification, ×400; scale bar, 50 μm. (B) Quantitative results of TUNEL assay showing apoptosis index of the four groups. Data are presented as mean±SEM. ****p<0.0001 compared with the Control (CON) group, ####p<0.0001 compared with the SU5416 (SU) group. n=3. (C) Representative results of active caspase-3 and PCNA as determined by western blotting. hUC-MSCs inhibited increased levels of active caspase-3 but not affect proliferation in the SU5416-treated models.

AKT and their active forms p-VEGFR2, p-AKT by western blot to determine whether VEGF-VEGFR2-AKT pathway-related molecules have changed in the hUC-MSCs transplantation group so further affect cell survival and apoptosis. The results showed that, compared with the SU5416 group, p-VEGFR2 and p-AKT were significantly increased in the SU5416+MSC group, which was comparable to the Control group (Fig. 5), indicating that hUC-MSCs intervention could activate the VEGF-VEGFR2-AKT pathway to induce the survival of lung cells and inhibit apoptosis.

Expression of pro-inflammatory cytokines in lungs of experimental rats

We examined the mRNA and protein expression of pro-inflammatory cytokines using RQ-PCR and ELISA. There was no significant difference in IL-1β, IL-6 or TNFα expression in both mRNA and protein levels among four groups (Fig. 6).

Discussion

So far, various animal models have been established to try to replicate human COPD. However, based on ex-

tensive literature reviews, there is currently no available model that can fully mimic the characteristics of human COPD (18). Therefore, it is necessary to establish specific models to mimic different subtypes of human COPD.

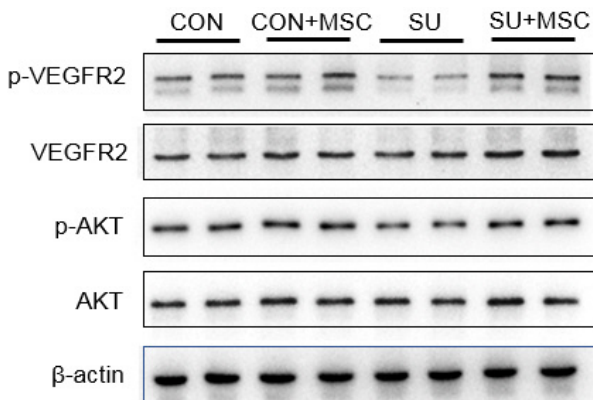


Fig. 5. hUC-MSCs rescued the expression of p-VEGFR2 and p-AKT in emphysema induced by SU5416. The protein expressions of p-VEGFR2, VEGFR2, p-AKT and AKT in the lungs were determined by western blotting. Compared with the control group (CON), p-VEGFR2 and p-AKT in the model group (SU) were significantly reduced, but both of them in the hUC-MSCs transplantation group (SU+MSC) returned to the level of the Control group. There was no significant change in the expression of VEGFR2 and AKT in each group.

Until now, four models have been established that confirmed the development of emphysema in mice/rats lack of significant inflammatory response (17-20). The first model was induced by subcutaneous administration of SU5416 (17), the second model used a single intratracheal injection of active caspase-3 (19), the third model was reproduced with intra-tracheal instillation of ceramide (20), a recent model was induced by NO₂ chronic exposure (18), all the four models caused non-inflammatory emphysema, and the first three models also caused lung cell apoptosis. Inflammation is one of the important mechanisms involved in COPD. However, because many patients with severe inflammatory lung diseases such as pneumonia and adult respiratory distress syndrome do not develop significant emphysema, inflammation cannot fully explain the loss of alveolar septa in emphysema. Apoptosis can directly cause emphysema, at least in animal models. In order to better study the anti-apoptotic effect of hUC-MSCs in emphysema, we used the first model by SU5416. We detected the gene level and protein level of pro-inflammatory factors. Compared with the Control group, we did not observe the significant change of pro-inflammatory cytokines (IL-1 β , IL-6 or TNF α) with SU5416 administration in model group. Similarly, hUC-MSCs had no significant effect on inflammatory response in normal or damaged lung tissues. These evi-

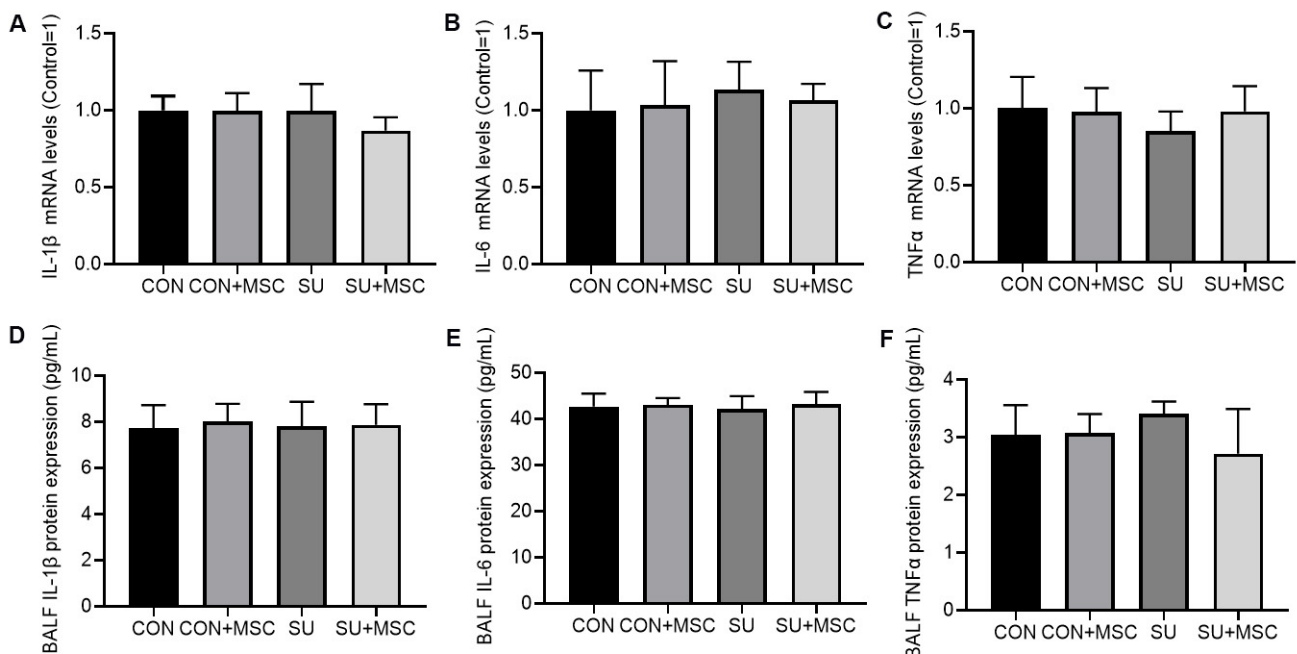


Fig. 6. hUC-MSCs did not alter the expression of pro-inflammatory cytokines in SU5416-induced emphysema. (A~C) RQ-PCR detect IL-1 β , IL-6 and TNF α mRNA expression in lungs, respectively. (D~F) ELISA detect IL-1 β , IL-6 and TNF α protein expression in BALF, respectively. hUC-MSCs had no significant effect on inflammatory response in normal or damaged lung tissues.

dences further showed that hUC-MSCs alleviated SU5416-induced emphysema by inhibiting apoptotic pathway rather than inflammatory pathway. This phenomenon that SU5416 induced emphysema may be directly caused by apoptosis. After apoptosis, due to the limited release of intracellular contents, it is not expected to lead to immune responses.

MSCs infused through the veins are mainly retained in the lungs, which provides an effective rationale for treatment of lung diseases including COPD and emphysema. hUC-MSCs have several attractive advantages for clinical use including they can be obtained without any invasiveness, can be efficiently expanded in labs, have lower immunogenicity, grow more rapidly, have faster doubling times and show a lower risk of infection. Moreover, hUC-MSCs have stronger effects in secretion of growth factor, immune regulation and anti-inflammation activity (21-24). However, only a few studies have explored application of hUC-MSCs in COPD. Notably, these studies did not explore the role of hUC-MSCs in opposing apoptosis in COPD or emphysema. The present study provides the first evidence that hUC-MSCs transplantation could repair the SU5416-induced emphysema by inhibiting apoptosis via rescuing VEGF-VEGFR2-AKT pathway.

Apoptosis of pulmonary parenchymal cells is implicated in pathogenesis of pulmonary emphysema both in human patients and animal models. Increased apoptosis and increased activity of caspase-3 have been reported in lungs of emphysema patients (25, 26). More directly, in animal models, intratracheal administration of active caspase-3 could cause lung cell apoptosis and emphysema (19), and treatment with caspase inhibitor reduced the SU5416-induced apoptosis-dependent emphysema (17). These findings show that lung cell apoptosis plays a critical role in pathogenesis of emphysema. In the SU5416-induced emphysema models used in this study, increased apoptosis was observed by TUNEL assay and active caspases-3 activity. After infusing hUC-MSCs, excessive apoptosis and increased active caspase-3 were reduced to the normal level, suggesting hUC-MSCs have great ability of opposing apoptosis.

We further studied the mechanism of hUC-MSCs inhibiting apoptosis, and found that the VEGF-dependent signaling pathway plays a key role in inhibiting apoptosis. The survival signal mediated by VEGF and its receptor VEGFR2 is essential for the survival of endothelial cells and the maintenance of the vascular system. Decreased expression of VEGF and VEGFR2 in emphysematous lungs are related to increased endothelial cell death. Damage of pulmonary vascular bed is a key feature in emphysema.

VEGF is a main and effective modulator of angiogenesis and a trophic factor required for survival of endothelial cells (27). The lung contains the highest level of VEGF expression among normal organs. VEGF in lung plays a key role in maintaining homeostasis of alveolar compartment. Recent studies involving emphysema patients and animal experiments reported that the damage of VEGF signaling was associated with pathogenesis of emphysema. Kasahara et al. and Kanazawa et al. reported that the expression of VEGF in lungs and induced sputum were significantly low in patients with emphysema (25, 28). Animal experiments showed that lung-targeted VEGF reduction led to increased alveolar cell apoptosis and emphysema (29, 30). VEGF is a well characterized anti-apoptotic growth factor. Some studies have reported that VEGF inhibits endothelial cell apoptosis *in vitro* (31, 32). VEGF specifically binds to VEGFR2 receptor (Flk-1/KDR) and subsequently activates PI3-kinase/Akt pathway (33). As a result, Akt inhibits caspase-9 and BAD expression (34, 35). In the VEGF-mediated signaling pathway, AKT acts as a key regulator, regulating cell survival, proliferation, and angiogenesis (36). In the lung, the induction of Akt expression have a variety of beneficial effects on cells, especially for the survival of alveolar cells (37). The reduction of VEGF/VEGFR2 expression can lead to endothelial cell apoptosis, which leads to emphysema changes (29, 38, 39). In this study, we used SU5416 to specifically inhibit VEGFR2 and block VEGF-VEGFR2 signal transduction, which resulted in emphysema changes. Compared with the Control group, VEGF, p-VEGFR2, and p-AKT were significantly reduced, accompanied by increased active caspase-3 and increased TUNEL-positive cells in the lungs of the emphysema, indicating that inhibition of VEGFR2 by SU5416 would lead to weakening of the VEGF-VEGFR2-AKT cascade, and further lead to the weakening of AKT-mediated survival signals and the increase of apoptosis. Studies have shown that VEGF can up-regulate the expression of VEGFR2 (40), which may promote the positive feedback of the VEGF-VEGFR2 signaling pathway. In this study, hUC-MSCs transplantation could rescue the expression of VEGF in the lung and restore it to the healthy level. At the same time, the levels of p-VEGFR2, p-Akt proteins involved in the VEGF signaling cascade were up-regulated to control levels, and cell apoptosis was effectively suppressed accompanied by emphysema damage was repaired, as seen in healthy lungs.

In summary, this study reports the role of hUC-MSCs in repairing of emphysema by inhibiting apoptosis via rescuing VEGF-VEGFR2-AKT pathway, for the first time. This study provides a basis for application of hUC-MSCs

in repairing emphysema and COPD.

Acknowledgments

This study was supported by the Youth Medical Talents Project of “Ke Jiao Qiang Wei” project of Jiangsu province (Grant number: QNRC2016449) and the “Innovative and Entrepreneurial Elite Team” Program (2016), Jiangsu, China.

Potential Conflict of Interest

The authors have no conflicting financial interest.

References

- Rabe KF, Watz H. Chronic obstructive pulmonary disease. *Lancet* 2017;389:1931-1940
- Matthay MA, Thompson BT, Read EJ, McKenna DH Jr, Liu KD, Calfee CS, Lee JW. Therapeutic potential of mesenchymal stem cells for severe acute lung injury. *Chest* 2010;138:965-972
- O'Reilly M, Thébaud B. Cell-based strategies to reconstitute lung function in infants with severe bronchopulmonary dysplasia. *Clin Perinatol* 2012;39:703-725
- Weiss DJ, Bertoncello I, Borok Z, Kim C, Panoskaltis-Mortari A, Reynolds S, Rojas M, Stripp B, Warburton D, Prockop DJ. Stem cells and cell therapies in lung biology and lung diseases. *Proc Am Thorac Soc* 2011;8:223-272
- Gu W, Song L, Li XM, Wang D, Guo XJ, Xu WG. Mesenchymal stem cells alleviate airway inflammation and emphysema in COPD through down-regulation of cyclooxygenase-2 via p38 and ERK MAPK pathways. *Sci Rep* 2015;5:8733
- Zhen G, Liu H, Gu N, Zhang H, Xu Y, Zhang Z. Mesenchymal stem cells transplantation protects against rat pulmonary emphysema. *Front Biosci* 2008;13:3415-3422
- Tibboel J, Keijzer R, Reiss I, de Jongste JC, Post M. Intravenous and intratracheal mesenchymal stromal cell injection in a mouse model of pulmonary emphysema. *COPD* 2014;11:310-318
- Bustos ML, Huleihel L, Kapetanaki MG, Lino-Cardenas CL, Mroz L, Ellis BM, McVerry BJ, Richards TJ, Kaminski N, Cerdene N, Mora AL, Rojas M. Aging mesenchymal stem cells fail to protect because of impaired migration and antiinflammatory response. *Am J Respir Crit Care Med* 2014;189:787-798
- Nagamura-Inoue T, He H. Umbilical cord-derived mesenchymal stem cells: their advantages and potential clinical utility. *World J Stem Cells* 2014;6:195-202
- Hao Y, Ran Y, Lu B, Li J, Zhang J, Feng C, Fang J, Ma R, Qiao Z, Dai X, Xiong W, Liu J, Zhou Q, Hao J, Li R, Dai J. Therapeutic effects of human umbilical cord-derived mesenchymal stem cells on canine radiation-induced lung injury. *Int J Radiat Oncol Biol Phys* 2018;102:407-416
Erratum in: *Int J Radiat Oncol Biol Phys* 2019;103:287
- Moroncini G, Paolini C, Orlando F, Capelli C, Grieco A, Tonnini C, Agarbati S, Mondini E, Saccomanno S, Goteri G, Svegliati Baroni S, Provinciali M, Introna M, Del Papa N, Gabrielli A. Mesenchymal stromal cells from human umbilical cord prevent the development of lung fibrosis in immunocompetent mice. *PLoS One* 2018;13:e0196048
- Liu L, Mao Q, Chu S, Mounayar M, Abdi R, Fodor W, Padbury JF, De Paepe ME. Intranasal versus intraperitoneal delivery of human umbilical cord tissue-derived cultured mesenchymal stromal cells in a murine model of neonatal lung injury. *Am J Pathol* 2014;184:3344-3358
- Shu L, Niu C, Li R, Huang T, Wang Y, Huang M, Ji N, Zheng Y, Chen X, Shi L, Wu M, Deng K, Wei J, Wang X, Cao Y, Yan J, Feng G. Treatment of severe COVID-19 with human umbilical cord mesenchymal stem cells. *Stem Cell Res Ther* 2020;11:361
- Le Thi Bich P, Nguyen Thi H, Dang Ngo Chau H, Phan Van T, Do Q, Dong Khac H, Le Van D, Nguyen Huy L, Mai Cong K, Ta Ba T, Do Minh T, Vu Bich N, Truong Chau N, Van Pham P. Allogeneic umbilical cord-derived mesenchymal stem cell transplantation for treating chronic obstructive pulmonary disease: a pilot clinical study. *Stem Cell Res Ther* 2020;11:60
- Cho JW, Park KS, Bae JY. Effects of Wharton's jelly-derived mesenchymal stem cells on chronic obstructive pulmonary disease. *Regen Ther* 2019;11:207-211
- Ridzuan N, Zakaria N, Widera D, Sheard J, Morimoto M, Kiyokawa H, Mohd Isa SA, Chatar Singh GK, Then KY, Ooi GC, Yahaya BH. Human umbilical cord mesenchymal stem cell-derived extracellular vesicles ameliorate airway inflammation in a rat model of chronic obstructive pulmonary disease (COPD). *Stem Cell Res Ther* 2021;12:54
- Kasahara Y, Tuder RM, Taraseviciene-Stewart L, Le Cras TD, Abman S, Hirth PK, Waltenberger J, Voelkel NF. Inhibition of VEGF receptors causes lung cell apoptosis and emphysema. *J Clin Invest* 2000;106:1311-1319
- Zhang Z, Wang J, Liu F, Yuan L, Ding M, Chen L, Yuan J, Yang K, Qian J, Lu W. Non-inflammatory emphysema induced by NO₂ chronic exposure and intervention with demethylation 5-Azacytidine. *Life Sci* 2019;221:121-129
- Aoshiba K, Yokohori N, Nagai A. Alveolar wall apoptosis causes lung destruction and emphysematous changes. *Am J Respir Cell Mol Biol* 2003;28:555-562
- Petrache I, Natarajan V, Zhen L, Medler TR, Richter AT, Cho C, Hubbard WC, Berdyshev EV, Tuder RM. Ceramide upregulation causes pulmonary cell apoptosis and emphysema-like disease in mice. *Nat Med* 2005;11:491-498
- Amable PR, Teixeira MV, Carias RB, Granjeiro JM, Borojevic R. Protein synthesis and secretion in human mesenchymal cells derived from bone marrow, adipose tissue and Wharton's jelly. *Stem Cell Res Ther* 2014;5:53
- Li X, Bai J, Ji X, Li R, Xuan Y, Wang Y. Comprehensive characterization of four different populations of human mesenchymal stem cells as regards their immune properties, proliferation and differentiation. *Int J Mol Med* 2014;34:695-704

23. Prasanna SJ, Gopalakrishnan D, Shankar SR, Vasandan AB. Pro-inflammatory cytokines, IFN γ and TNF α , influence immune properties of human bone marrow and Wharton jelly mesenchymal stem cells differentially. *PLoS One* 2010;5:e9016
24. Barcia RN, Santos JM, Filipe M, Teixeira M, Martins JP, Almeida J, Agua-Doce A, Almeida SC, Varela A, Pohl S, Dittmar KE, Calado S, Simoes SI, Gaspar MM, Cruz ME, Lindenmaier W, Graça L, Cruz H, Cruz PE. What makes umbilical cord tissue-derived mesenchymal stromal cells superior immunomodulators when compared to bone marrow derived mesenchymal stromal cells? *Stem Cells Int* 2015;2015:583984
25. Kasahara Y, Tuder RM, Cool CD, Lynch DA, Flores SC, Voelkel NF. Endothelial cell death and decreased expression of vascular endothelial growth factor and vascular endothelial growth factor receptor 2 in emphysema. *Am J Respir Crit Care Med* 2001;163(3 Pt 1):737-744
26. Demedts IK, Demoor T, Bracke KR, Joos GF, Brusselle GG. Role of apoptosis in the pathogenesis of COPD and pulmonary emphysema. *Respir Res* 2006;7:53
27. Ferrara N. VEGF: an update on biological and therapeutic aspects. *Curr Opin Biotechnol* 2000;11:617-624
28. Kanazawa H, Asai K, Hirata K, Yoshikawa J. Possible effects of vascular endothelial growth factor in the pathogenesis of chronic obstructive pulmonary disease. *Am J Med* 2003;114:354-358
29. Tang K, Rossiter HB, Wagner PD, Breen EC. Lung-targeted VEGF inactivation leads to an emphysema phenotype in mice. *J Appl Physiol* (1985) 2004;97:1559-1566; discussion 1549
30. Takahashi Y, Izumi Y, Kohno M, Ikeda E, Nomori H. Airway administration of vascular endothelial growth factor siRNAs induces transient airspace enlargement in mice. *Int J Med Sci* 2013;10:1702-1714
31. Gerber HP, Dixit V, Ferrara N. Vascular endothelial growth factor induces expression of the antiapoptotic proteins Bcl-2 and A1 in vascular endothelial cells. *J Biol Chem* 1998;273:13313-13316
32. Gupta K, Kshirsagar S, Li W, Gui L, Ramakrishnan S, Gupta P, Law PY, Hebbel RP. VEGF prevents apoptosis of human microvascular endothelial cells via opposing effects on MAPK/ERK and SAPK/JNK signaling. *Exp Cell Res* 1999;247:495-504
33. Gerber HP, McMurtrey A, Kowalski J, Yan M, Keyt BA, Dixit V, Ferrara N. Vascular endothelial growth factor regulates endothelial cell survival through the phosphatidylinositol 3'-kinase/Akt signal transduction pathway. Requirement for Flk-1/KDR activation. *J Biol Chem* 1998;273:30336-30343
34. Cardone MH, Roy N, Stennicke HR, Salvesen GS, Franke TF, Stanbridge E, Frisch S, Reed JC. Regulation of cell death protease caspase-9 by phosphorylation. *Science* 1998;282:1318-1321
35. del Peso L, Gonzalez-Garca M, Page C, Herrera R, Nunez G. Interleukin-3-induced phosphorylation of BAD through the protein kinase Akt. *Science* 1997;278:687-689
36. Shiojima I, Walsh K. Role of Akt signaling in vascular homeostasis and angiogenesis. *Circ Res* 2002;90:1243-1250
37. Prakash M, Kumar D, Kotnala S, Murali V, Kumar Tyagi A. Recombinant human keratinocyte growth factor induces Akt mediated cell survival progression in emphysematous mice. *Arch Bronconeumol* 2015;51:328-337
38. Giordano RJ, Lahdenranta J, Zhen L, Chukwueke U, Petrache I, Langley RR, Fidler IJ, Pasqualini R, Tuder RM, Arap W. Targeted induction of lung endothelial cell apoptosis causes emphysema-like changes in the mouse. *J Biol Chem* 2008;283:29447-29460
39. Petrache I, Fijalkowska I, Zhen L, Medler TR, Brown E, Cruz P, Choe KH, Taraseviciene-Stewart L, Scerbavicius R, Shapiro L, Zhang B, Song S, Hicklin D, Voelkel NF, Flotte T, Tuder RM. A novel antiapoptotic role for α 1-antitrypsin in the prevention of pulmonary emphysema. *Am J Respir Crit Care Med* 2006;173:1222-1228
40. Shen BQ, Lee DY, Gerber HP, Keyt BA, Ferrara N, Zioncheck TF. Homologous up-regulation of KDR/Flk-1 receptor expression by vascular endothelial growth factor in vitro. *J Biol Chem* 1998;273:29979-29985